Macromolecular Research, Vol. 22, No. 8, pp 832-842 (2014)
DOI 10.1007/s13233-014-2117-7

www.springer.com/13233
pISSN 1598-5032 eISSN 2092-7673

Synthesis of Alginate Based Silver Nanocomposite Hydrogels for Biomedical Applications

P. Rama Subba Reddy[1], K. Madhusudana Rao[2], K. S. V. Krishna Rao*[,1], Yury Shchipunov[3], and Chang-Sik Ha*[,2]

[1]*Department of Chemistry, Yogi Vemana University, Kadapa-516 003, India*
[2]*Department of Polymer Science and Engineering, Pusan National University, Busan 609-735, Korea*
[3]*Institute of Chemistry, Far East Department, Russian Academy of Sciences, Vladivostok, Russian Federation*

Received January 3, 2014; Revised April 5, 2014; Accepted May 6, 2014

Abstract: Sodium alginate and poly(acrylamide-*co*-*N*-vinylcaprolactam-*co*-acrylamidoglycolic acid) based dual responsive semi-IPN hydrogels (SA-PAVA) were successfully synthesized by free radical redox polymerization. *N*, *N*′-Methylene-bis-acrylamide was used as a crosslinker and 5-fluorouracil, an anti-cancer drug, was loaded onto these semi-IPN hydrogels *via* equilibrium swelling method. The hydrogels were also used as templates for the production of silver nanoparticles by using $NaBH_4$ as reducing agent. In order to understand the polymer-drug interactions, pristine, as well as drug loaded, SA-PAVA hydrogels were characterized by Fourier transform infrared spectroscopy and differential scanning calorimetry. The formation of silver nanoparticles was confirmed by UV-visible spectroscopy, thermogravimetric analysis (TGA), scanning electron microscopy (SEM) and transmission electron microscopy (TEM). The swelling behavior of the hydrogel was investigated in distilled water under various pH and temperature conditions. *In vitro* release of 5-fluorouracil from these SA-PAVA hydrogels was carried out in gastro-intestinal fluids different temperatures. The SA-PAVA hydrogel/silver nanocomposites showed excellent anti-bacterial activity towards *Escherichia coli* and *Bacilli*.

Keywords: semi-IPN hydrogels, silver nanocomposites, drug delivery, 5-fluorouracil, antimicrobial activity.

Introduction

The development of multi-functional intelligent hydrogels (MFIHs) has gaining momentum to obtain maximum therapeutic benefit in fundamental biomedical studies.[1,2] The medicinal interest in developing MFIHs largely stems from their convenient swelling properties in response to external stimuli, such as temperature, pH, ionic strength, light, electric and magnetic fields, *etc*.[3-6] Due to the presence of hydrophilic functional groups, such as hydroxyl, carboxylic, amide and sulfonic groups along with the polymer chains, hydrogels exhibit high hydrophilicity, biocompatibility and similarity to natural tissues.[7] Dual responsive or 'intelligent' hydrogels utilize integrated functionalities and perform controlled actions such as switching on/off drug release, signaling to the sensing device, recognizing a specific cell, and monitoring the concentration level in a biological and living system.[8-10] More specifically, ionic hydrogels are used to immobilize a drug delivery device on a specific site for targeted release and optimal drug delivery due to the intimacy and extended duration of contact.[11,12] To improve the response rate of hydrogels without decreasing their mechanical strength, introduction of semi-interpenetrating polymer network (semi-IPN) structure into the hydrogel networks has been developed.[13-17] Metal nanoparticles embedded in a hydrogel matrix are important for many applications. Generally solution-reduction chemistry that offers freely-diffusion-reaction of silver ions with a reducing agent leads to uncontrolled particle size formation. However, hydrogel network or polymeric matrix provides a way to controlled particle size and shape of silver nanoparticles in the hydrogel matrix.[18] Recent reports showed the hydrogels not only have been used for drug delivery applications but also useful for the production of size controlled silver nanoparticles. The multifunctional hydrogels with incorporating silver nanoparticles exhibited excellent antibacterial activity and have been used especially for wound dressing and water purification purposes.[19,20]

Sodium alginate (SA) is one of the most abundant and naturally occurring polysaccharides. SA has received considerable attention for its use in pharmaceutical dosages forms, particularly as a vehicle for controlled drug delivery due to its biocompatibility, biodegradability, high hydrophilicity, and mechanical strength.[21-24] Poly(*N*-vinyl caprolactam), PNVC,

*Corresponding Authors. E-mails: csha@pnu.edu or drksvkrishna@yahoo.com, ksvkr@yogivemanauniversity.ac.in

and poly(acrylamidoglycolic acid), PAGA, were chosen as a model system due to their biocompatibility. PNVAC hydrogel has a swelling and shrinking temperature near the body temperature and PAGA has sensitivity at gastro-intestinal fluids. PNVC and PAGA were also expected to be suitable for developing new separation systems to complement traditional precipitation, chromatography, and extraction of biological molecules and controlled release of bioactive agents.[14,25-28]

The development of MFIHs requires both engineering design of a network and biomedical tuning of intelligent responses. Hence, based on above mentioned polymers and their properties, we synthesized a new MFIH system with dual (temperature and pH) responsive properties from sodium alginate/poly(acrylamide-*co*-*N*-vinyl caprolactam-*co*-acrylamidoglycolic acid) semi-IPN hydrogels (SA-PAVA) by free radical copolymerization. An effective strategy of introducing semi-IPN structure was also developed to improve the response rate of the hydrogels without decreasing the mechanical strength. 5-Fluorouracil (5-FU) is commonly used as an anticancer drug for the treatment of solid tumors of breast, stomach, colon and pancreas.[29-32] It has been widely used in drug administration due to its large number of secondary effects that accompany its conventional administration. Though it is used extensively in cancer chemotherapy,[32] however, the drug exhibits high toxicity and can cause side effects.[33] In the treatment of stage III colorectal cancer called FOLFOX, there is need of infusion of 5-FU for 22 h. This long duration of infusion results in a few side effects including the metallic taste appearing during the infusion hours. Due to this drawback, controlled delivery is essential for the treatment of 5-FU which reduces the frequency of dosing, In addition, the need of infusion will not be there by the controlled delivery. In the case of simple hydrogel containing 5-FU, however, the drug release will be fast which will not give controlled release. In the present study, we utilized MFIHs for the encapsulation of 5-FU as a model drug. The MFIHs could be effectively useful for colon cancer drug delivery in order to enhance the drug release in alkaline conditions and minimize it in the gastric region. The MFIHs were also used as templates for the production of silver nanoparticles in the hydrogels. Owing to the presence of highly hydrophilic functional groups in hydrogels, silver nanoparticles were easily formed in a controlling size and shape. These hydrophilic functional groups could anchor more silver ions, and then the anchored silver ions would be reduced in the presence of sodium borohydride. The formed silver nanomaterials could be more stable in the hydrogel networks owing to more favorable hydrogen bonding interactions between hydrogel chains, which reduce the repulsive interaction between neighboring silver nanoparticles in the hydrogel networks. The developed semi-IPN system could be advantages because the system exhibited dual responsive properties with high swelling capability. Hence, the semi-IPN hydrogels can be applied for both localized drug delivery as well as antibacterial applications. Furthermore, the presence of silver nanomaterials in the hydrogels could be able to enhance the controlled release properties of 5-FU.

Experimental

Materials. Analytical reagent grade samples of sodium alginate (SA), acrylamide (Am), *N*-vinylcaprolactam (NVC), acrylamidoglycolic acid (AGA), *N*,*N*′-methylene-bis-acrylamide (BAm), *N*,*N*,*N*′,*N*′-tetramethylethylene diamine (TEMED), potassium persulfate (KPS) and 5-Fluorouracil (5-FU) were purchased from Aldrich. All chemicals were used as received and double distilled (DD) water was used throughout the experiments.

Preparation of SA-PAVA Hydrogels. Semi-IPN hydrogels of SA/poly(Am-*co*-NVC-*co*-AGA) were prepared by a radical copolymerization. Monomers were dissolved in 2.5 mL of 2 wt% SA solution. To this mixture, 1.0 mL (8.1×10^{-4} mol) of crosslinking agent (BAm, 1 wt% aqueous solution), 1.0 mL (3.7×10^{-3} mol) of KPS (5 wt% aqueous solution) and 1.0 mL of TEMED (1 wt% aqueous solution) were added. Polymerization reaction was carried out in petri dishes, with maintaining at 45 °C for 7 h. After the polymerization, hydrogels obtained were cut into disks of 1.5 mm diameter and washed with DD water to remove unreacted reagents and then dried under vacuum until attainment of constant mass. The completion of polymerization and of monomer conversion was confirmed gravimetrically. The SA-PAVA hydrogels were prepared by varying the fractions of AGA, NVC, and BAm (See Table I).

Preparation of SA-PAVA Hydrogel/Silver Nanocomposites (SNC). SA-PAVA based SNC hydrogels were prepared by incorporating dry SA-PAVA hydrogel disks into DD water and equilibrated for 4 days. These gels were transferred to brown air-tight test bottles containing 50 mL of aqueous $AgNO_3$ solution and then allowed to equilibrate for 1 day. This step allows the transfer of silver ions present in solution to the hydrogel networks by ion exchange process. The silver salts presented in SA-PAVA hydrogel were reduced by $NaBH_4$ for 2 h in order to reduce the silver ions into silver nanoparticles. The developed SNC SA-PAVA hydrogels were named as SA-PAVA-Ag.

Swelling Experiments. The % swelling fraction (% SF) and the % equilibrium swelling (% ES) were calculated as:

$$\% \text{ Swelling fraction} = \left[\frac{m_t - m_d}{m_d}\right] \times 100 \quad (1)$$

$$\% \text{ Equilibrium swelling} = \left[\frac{m_\infty - m_d}{m_d}\right] \times 100 \quad (2)$$

where m_t and m_d are mass of swollen SA-PAVA hydrogels for a given time t and dried SA-PAVA hydrogels, respectively. Here, m_∞ is the equilibrium mass of swollen SA-PAVA hydrogels. Kinetic and equilibrium swelling experiments on SA-PAVA hydrogels of this study have been performed in DD water and different pH solutions (1.0, 3.0, 5.0, 7.0, and 9.0) at 30 °C (±0.5 °C).

Encapsulation Efficiency of SA-PAVA Hydrogels. 5-FU was encapsulated into SA-PAVA hydrogels by a swelling equilibrium method. The hydrogels were immersed in known concentration of drug solution and allowed them to swell for 24 h at 37 ºC. The solubility of 5-FU in DD water is 13 mg/mL, which in general is quite low. However, sodium salt can enhance the solubility of 5-FU upto 65 mg/mL.[14] In order to load the high amount of drug content into the polymeric network, gel disks were immersed in a sodium salt of 5-FU aqueous solution. Equilibration process allows adsorption of 5-FU that is present with the SA-PAVA hydrogels in the solvent. The loading efficiency of 5-FU in the SA-PAVA hydrogel was determined UV-Visible spectrophotometer (DS 8000, LABINDIA, India.). 5-FU loaded hydrogel was placed in 50 mL of buffer (pH=7) solution and stirred vigorously for 48 h to extract 5-FU from the hydrogels. The solution was filtered and assayed by an UV-Visible spectrophotometer at a fixed wavelength (λ_{max}= 270 nm). % of 5-FU loading and the encapsulation efficiency (EE) of SA-PAVA hydrogels was calculated by the following eqs. (3) and (4), and the resulting data was compiled in Table I.

$$\% \text{ Drug loading} = \frac{\text{Amount of drug in the SA-PAVA hydrogels}}{\text{Amount of SA-PAVA hydrogels}} \times 100 \quad (3)$$

$$\% \text{ Encapsulation efficiency} = \frac{\text{Actual drug loading}}{\text{Theoretical drug loading}} \times 100 \quad (4)$$

***In vitro* Release Studies.** *In vitro* drug release experiments were carried out using the dissolution system (DS8000, LABINDIA, India) equipped with eight baskets. Drug release rates were measured at 37 ºC under 100 rpm speed. Drug release kinetics was analyzed by plotting the % cumulative release data (M_t/M_∞) versus time. The SA-PAVA hydrogels were studied in buffer medium at pH=7.4 and pH=1.2, as well as at 25 and 37 ºC for formulation A.

Antibacterial Studies. Nutrient agar medium was prepared by mixing peptone (5 g), beef extract (3 g), and NaCl (5 g) and the pH of the solution was adjusted to 7. Then, 15 g of agar was added to the above mixture. The agar medium was sterilized in a conical flask at a pressure of 15 lbs for 30 min. This medium was transferred into sterilized petri dishes in a laminar air flow. After solidification of the agar media, *Escherichia coli* and *Bacilli* were spreaded over the solid surface of the media. To this inoculated petri dish, one drop of SA-PAVA-Ag particle solution (20 mg/10 mL DD water) was added using a 50 μL tip and incubated for 48 h at 37 ºC.

Characterization. Fourier transform infrared spectroscopy (Perkin Elmer Spectrum Two, UK) analysis was performed to identify the chemical structure of the SA-PAVA hydrogels. Furthermore, to investigate the drug nature in the hydrogel matrix, differential scanning calorimetry (DSC) (Model-SDTQ600, USA) analysis was preformed for pure drug, 5-FU loaded SA-PAVA hydrogel, and pristine SA-PAVA hydrogel. Thermogravimetric analysis (TGA) (Model-SDTQ600, USA) was performed for pristine SA-PAVA and SA-PAVA-Ag nanocomposites. Analysis of the samples was performed at a heating rate of 10 ºC/min under N_2 atmosphere with a purging rate of 100 mL/min. UV-visible spectroscopy of SA-PAVA-Ag nanocomposite (10 mg in 1 mL of distilled water) was recorded on an UV-Spectrophotometer (LABINDIA-3092, India). Morphology of the SA-PAVA hydrogels was recorded using a scanning electron microscope (SEM) (MERA\\TESCAN). 10 mg/mL powdered sample of SA-PAVA hydrogel was dispersed in DD water under constant stirring. This dispersion was placed on a 400 mesh copper grid and allowed to air dry for 5 min. Transmission electron microscopy (TEM) images of the silver particles were taken on a Tecnai T-12 microscope operated at 80 kV (FEI, Camebridge, England).

Results and Discussion

Dual (temperature and pH) responsive SA-PAVA semi-IPN hydrogels were prepared by random free radical polymerization with sequential crosslinking method. Simple combination of sodium alginate (SA), *N*-vinyl caprolactam (NVC) and acrylamidoglycolic acid (AGA) by the formation of new materials with the versatile advantages, such as temperature sensitivity of NVC, pH sensitivity of AGA and excellent mechanical properties of SA. The monomers were initiated by a redox pair, TEMED and APS,[14] crosslinked by BAm in the presence of hydrophilic SA. The digital photographs of SA-PAVA semi-IPN hydrogels are shown in Figure 1. In this study, semi-IPNs were not only used for the controlled release of 5-FU but also used as templates for the preparation of stable silver nanoparticles in the hydrogel networks. The schematic representation of dual responsive controlled release of 5-FU and the formation of silver nanoparticles in the hydrogel networks are presented in Scheme I.

FTIR Analysis. FTIR spectra of pristine SA-PAVA hydrogel, 5-FU, and drug loaded SA-PAVA hydrogel are presented in Figure 2. Two peaks around 1663 and 1608 cm^{-1} are due to

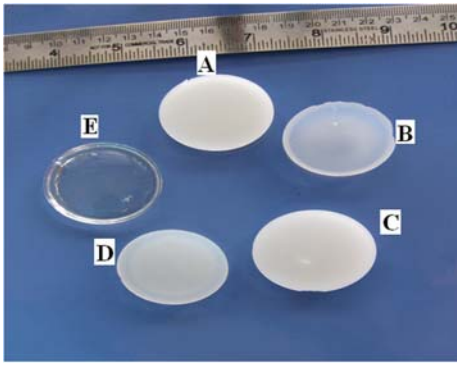

Figure 1. Digital photographs of hydrogels with various formulations.

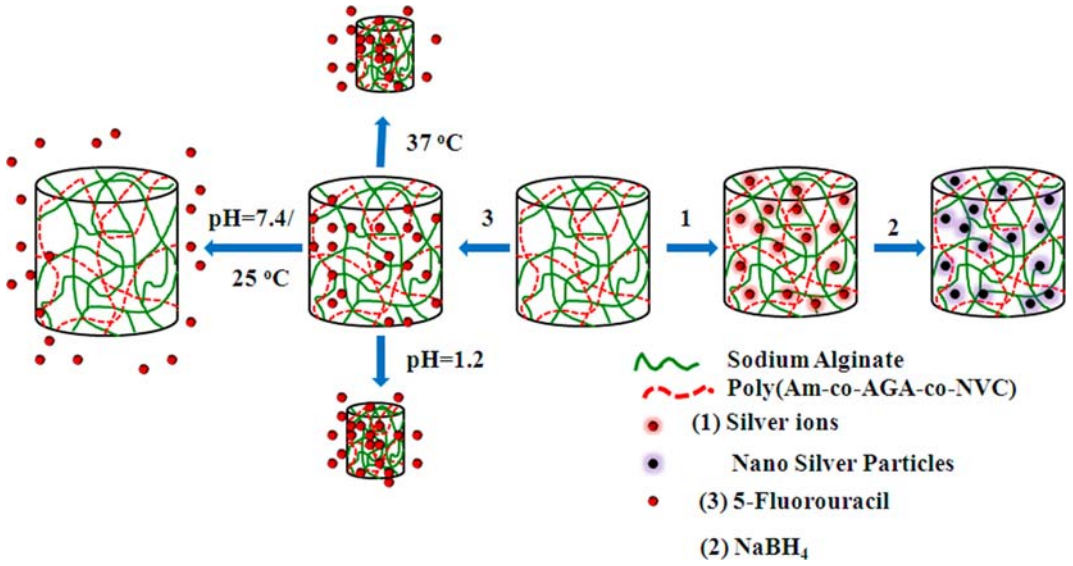

Scheme I. Schematic representation of SA/poly(Am-*co*-AGA-*co*-NVC) semi-IPN hydrogels.

amide-I and amide-II of acrylamide units while C-N and C-H stretching bands appear at 1440 and 2922 cm^{-1}, respectively, further confirm the presence of amide groups. A broad band observed between 3600 and 3000 cm^{-1} is due to the overlapping of the O-H stretching bands of carboxylic acid and O-H group of alcohol of AGA, SA and N-H of the amide groups.

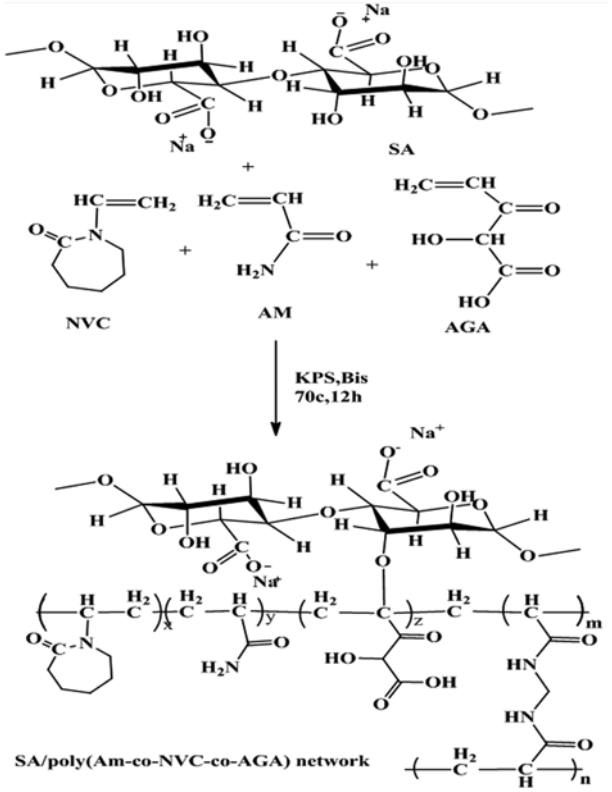

Scheme II. Schematic representation of drug release mechanism and silver composite formation of SA/PAVA semi-IPN hydrogel.

Moreover, a band is observed at 1694 cm^{-1} due to the presence of COO^- of AGA and SA in the spectrum of SA-PAVA hydrogel in addition to a band at 1641 cm^{-1}. Schematic representation of crosslinking reaction of SA-PAVA hydrogel is presented in Scheme II.

Based on the molecular structure of 5-FU, it acts chemically as either proton acceptor (through -C=O groups) or proton donor (through -NH groups). Also SA-PAVA hydrogels has proton acceptor (carbonyl group, -C=O), amine groups functioning as the proton donor (Figure 2). The stretching vibration bands are attributed to the functionalities of carbonyl (1706 cm^{-1}) and amine (3354 and 3374 cm^{-1}) groups of the molecularly dispersed 5-FU associating with SA-PAVA hydrogels through H-bonds.

DSC Studies. To investigate the physical nature of the 5-FU in the SA-PAVA hydrogel network, DSC was chosen as a

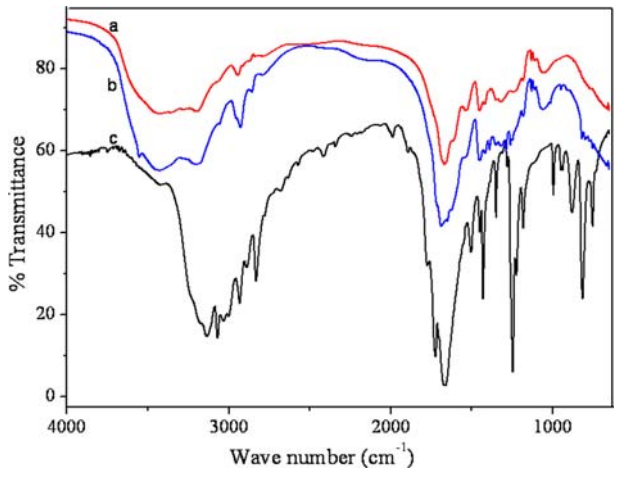

Figure 2. FTIR spectra of (a) pure gel, (b) drug loaded gel, and (c) pure drug for formulation A.

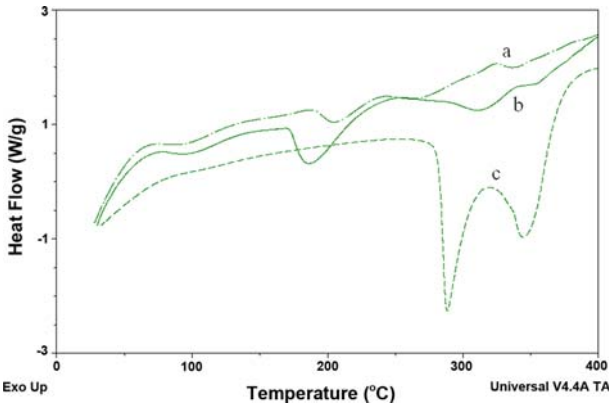

Figure 3. DSC thermograms of (a) pure hydrogels, (b) drug-loaded hydrogels, and (c) 5-FU for the formulation A.

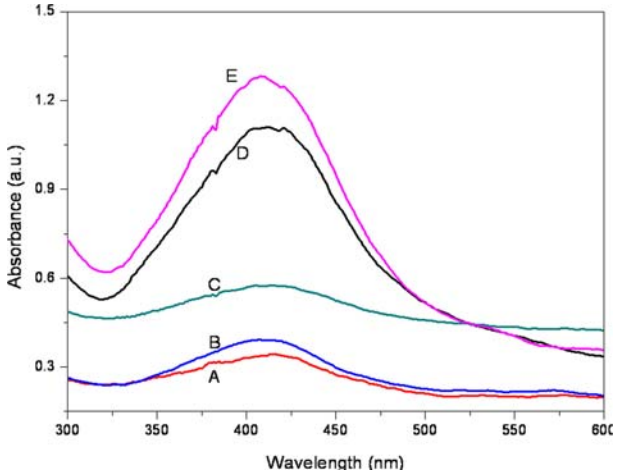

Figure 4. UV-absorption of (SA-PAVA) silver nano particles samples; Formulations A, B, C, D, and E are listed in Table I.

complementary technique. DSC curves of pure 5-FU, 5-FU loaded SA-PAVA hydrogel, and pristine SA-PAVA hydrogel are depicted in Figure 3. 5-FU shows a sharp peak at 285.16 °C due to polymorphism and melting, but no characteristic peak is observed at 285.16 °C for 5-FU loaded hydrogels. It may be due to the molecular level dispersion of 5-FU in SA-PAVA hydrogel network. The 5-FU molecules seem to be masked with SA-PAVA polymer chains.

UV-Visible Spectra. Fabrication of silver nanoparticles in the network of SA-PAVA hydrogel can be expected in our present method, due to the silver salts embedded in SA-PAVA hydrogels that are readily reduced by $NaBH_4$, which are immediately turn into brown color. It indicates that the silver nanoparticles were formed and entrapped inside the polymeric SA-PAVA hydrogel networks. The presence of silver nanoparticles in the hydrogel network was confirmed by using UV-Visible spectrophotometer. Figure 4 shows UV-Visible spectra of SA-PAVA-Ag hydrogels. The surface plasmon resonance band observed at 420 nm confirmed the formation of silver nanoparticles in the hydrogel networks.

TGA Studies. The thermal stability of hydrogels with combining sodium alginate and all functional monomers (pristine SA-PAVA hydrogel and SA-PAVA-Ag) were investigated by TGA (Figure 5). Figure 5 shows the % decomposition of the hydrogel and the SNC hydrogel. First step decomposition is attributed to the weight loss of residual moisture and the gel has initial decomposition of the hydrogel chains that occurred around 230 °C. 80% weight loss occurred at 450 °C for both hydrogel and SA-PAVA-Ag hydrogel. A clear difference has been observed in TGA experiments in that SA-PAVA-Ag hydrogel exhibits better thermal stability than the pristine hydrogel. The difference in the decomposition between the hydrogel and the silver nanocomposite hydrogel with the formulation A was found to be 5.5%, which indicates the formation of silver nanoparticles in the hydrogel was about 5.5%, whereas the formation of silver nanoparticles in other SA-PAVA hydro-

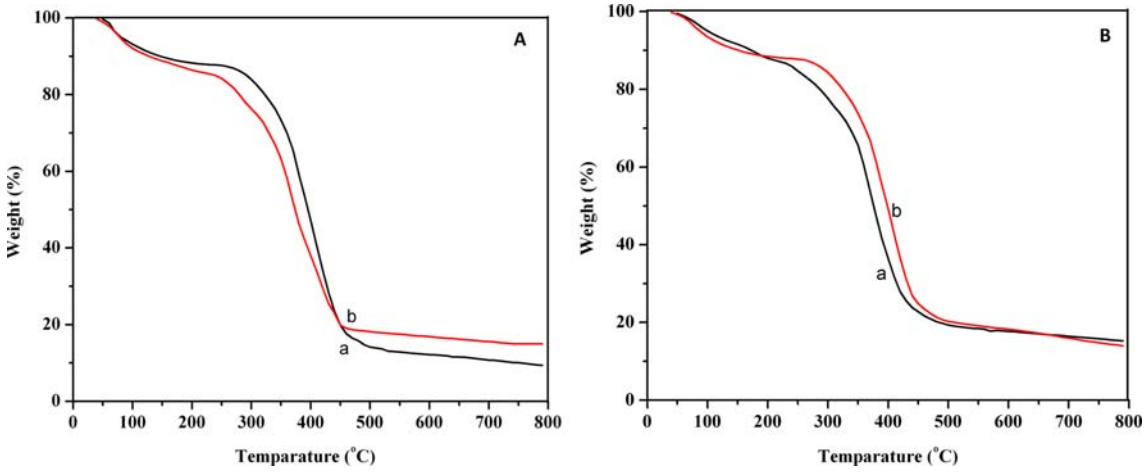

Figure 5. Thermogravimetric analysis curves of pure hydrogels (a) and silver composite of (b) SA-PAVA semi-IPN hydrogel for formulation A.

gels with different formulations was about 2.6%, 3.6%, 3.62%, and 3.9%, respectively (See Supporting Information). Among all formulations the highest amount of silver nanoparticles were formed in the formulation A hydrogel. Based on these results, the optimized amount of silver nanoparticles formed could be said to be about 5.5% in the hydrogels. Figure 5(B) shows TGA curves of (a) drug loaded SA-PAVA-Ag, and (b) SA-PAVA-Ag hydrogels after dissolving 5-FU. The results showed that the weight loss of silver nanoparticles was observed about 0.8% after exposing to external stimuli. The results indicate that the silver nanoparticles were released for long time when exposing to external stimuli. This is due to the fact that hydrogels contain many hydrophilic functional groups, which are responsible to decrease the interaction between silver nanoparticles owing to more favorable interactions between hydrogel chains. Thus the silver nanoparticles are more stable in hydrogel networks. The hydrogels might be effectively useful for silver releasing wound dressing applications.

SEM and TEM Studies. SEM images of pristine SA-PAVA hydrogels as well as SA-PAVA-Ag nanocomposite hydrogels are shown in Figure 6(a) and (b), respectively. The pristine hydrogel showed a smooth surface (a), whereas silver embedded SA-PAVA hydrogel showed a clear formation of silver nanoparticles in hydrogel network structures without forming aggregation (b). The high resolution SEM images of silver nanoparticles showed individual nanoparticles with about 20 nm in size (Figure 7(a)). TEM images of the SA-PAVA silver nanocomposite shown in Figure 7(b) and (c) indicate that the particles are well dispersed, spherical in shape with a narrow size distribution with an average diameter of 20 nm in size. Moreover, the electron diffraction pattern of Ag nanoparticles is clearly visible in Figure 7(d) as three diffraction rings belonging to (111), (200), and (220) reflections, indicating the formed silver nanoparticles are crystalline and have a face centered cubic (fcc) structure.

Swelling and Deswelling Studies. The percentage of swelling and deswelling kinetic curves of the SA-PAVA hydrogels with different SA, AGA, NVC and BAm contents are shown in Figure 8. The swelling data shows that the rate of % of swelling ratio is increased with increasing amount of anionic content in the SA-PAVA hydrogel network and decreased with increasing crosslinker content (BAm) from 8.1×10^{-4} to 9.7×10^{-4} mol%. The hydrogel with 8.1×10^{-4} mol% of BAm has the swelling fraction about 225% within 10 h, whereas the hydrogel with 9.7×10^{-4} mol% of BAm has about 175%, within the same time frame. Before the swelling in the dry SA-PAVA hydrogel, there are strong intermolecular interactions, such as hydrogen bonding and hydrophobic interactions, which remain in a glassy state.[34] The above behavior suggests that a glassy inner core might exist in the dry hydrogel having a higher crosslinking.

To understand the water retention capacity of the SA-PAVA hydrogels synthesized by the redox polymerization with BAm as crosslinker, the water-retention properties of the crosslinked copolymers were measured by deswelling kinetic experiments at 25 ºC (Figure 8(b)). Equal masses of swollen hydrogels were taken in weighing pans, and the mass loss of water of the swollen hydrogels was estimated by gravimetric method at different time intervals. The initial stage of deswelling kinetics indicated that the less crosslinked hydrogels had higher loss of water content. This type of nature of hydrogel deswelling or collapse has been ascribed to the formation of an ion-cluster. This is due to the dependence on solvent polarity and polymer charge density, as has been theoretically predicted.[14] The above results give the information that the deswelling rates were slower and water retention capacity was higher for the SA-PAVA hydrogel crosslinked by higher contents of BAm. In the case of monomers variation, the swelling of the hydrogels increases with increasing contents of AGA and NVC. This is because of improved hydrophilic functional groups of

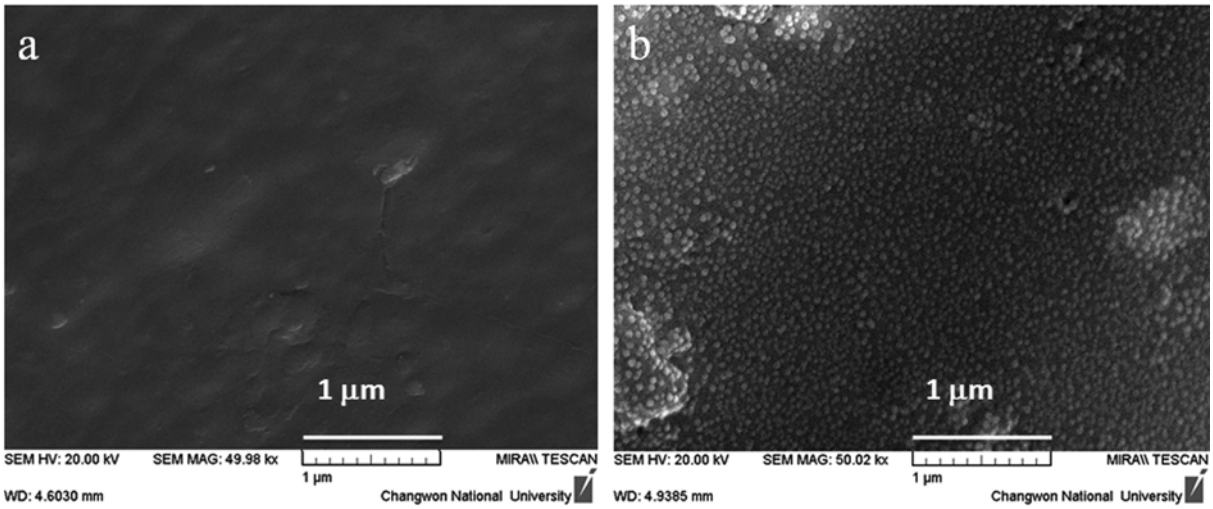

Figure 6. Scanning electron microphotographs of (a) SA-PAVA semi-IPN hydrogel, (b) silver composite of SA-PAVA semi-IPN (a, X49.98 k; b, X50.02 k).

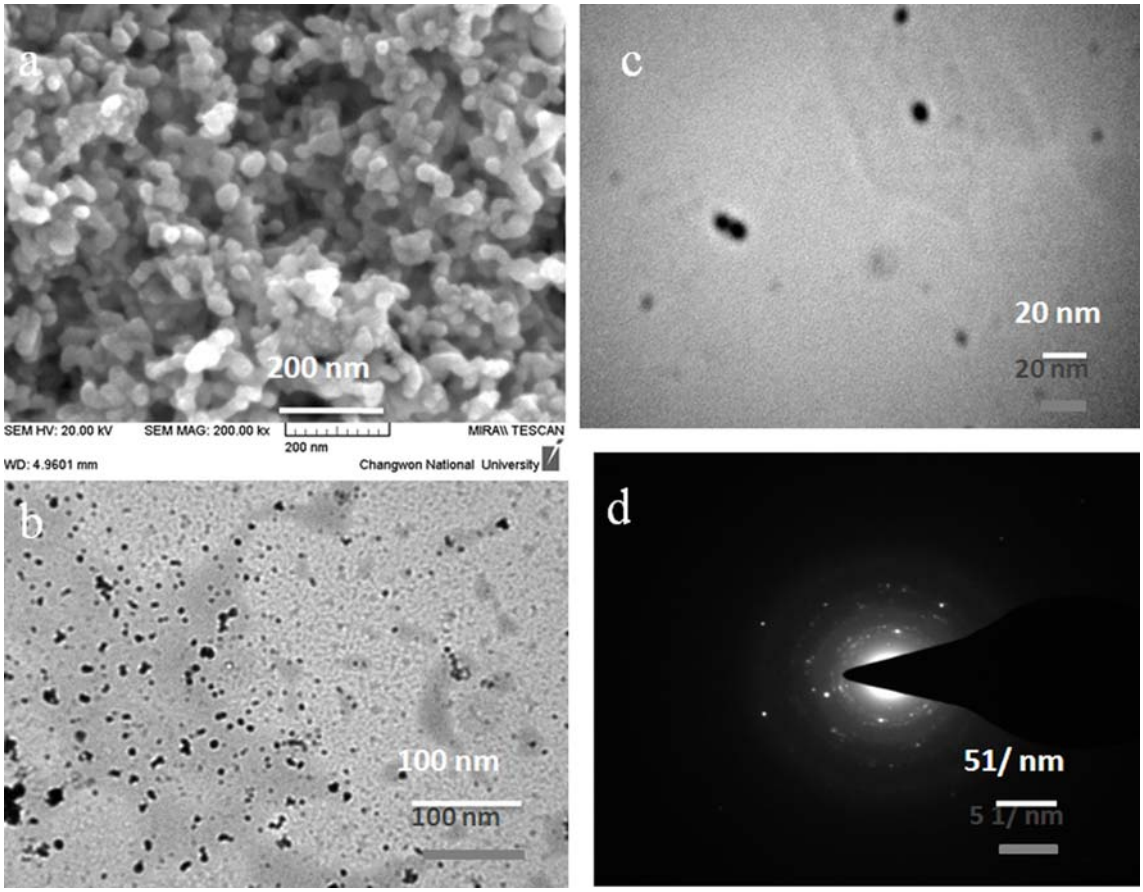

Figure 7. SEM images of (a) silver nanoparticles in SA-PAVA semi IPN (a, X200.0k), TEM images of (b) SA-PAVA silver composite hydrogels low resolution, (c) high resolution, and (d) EDS pattern of silver nanoparticles for formulation A.

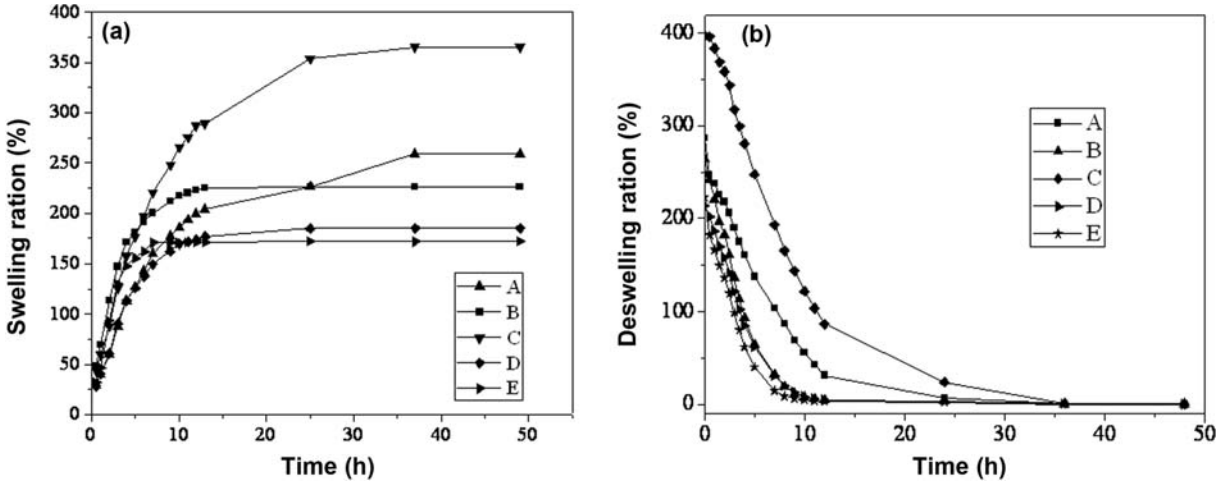

Figure 8. (a) Swelling and (b) deswelling ratio of SA-PAVA semi-IPN hydrogels.

the hydrogel. Among all the compositions the hydrogel C showed better swelling due to the absence of NVC and next follow the hydrogel B due to the absence of AGA, but in the presence of both NVC and AGA the hydrogel D exhibited the less swelling than the hydrogel B and C, which is attributes to higher concentration of BAm due to the complexation as well as the strong intermolecular hydrogen boding interactions.

To study the water diffusion capacity of SA-PAVA hydrogels, primary swelling data were fitted to the following Pep-

pas equation.[14]

$$\frac{m_t}{m_\infty} = kt^n \quad (5)$$

where m_t and m_∞ are the amount of water absorbed by the SA-PAVA hydrogel at time t and at equilibrium, k is a specific constant of the hydrogel, and n is a specific exponent of the mode of transport of the penetrate. The n, k and r values of SA-PAVA hydrogels are given in Table I. For the first case, n=0.5, corresponding to a Fickian diffusion, the rate of diffusion is much slower than the rate of relaxation. For the second case, n=1, the diffusion is very fast, contrary to the rate of relaxation, and the third case corresponds to an anomalous diffusion or non-Fickian diffusion with n values from 0.55 to 0.99. A slight variation of the diffusion exponent with SA content is observed, but mostly n is close to 0.5 though they are not exactly equal to 0.5. It can be said that the overall process is quasi-Fickian diffusion with partly anomalous behavior, that is, chain relaxation controlled process of SA-PAVA hydrogels. The slight anomalous behavior may be due to the regularity of the chain and strong inter chain interactions *via* the formation of hydrogen bonding, leading to a squeeze structure that would emphasize the anomalous aspects of diffusion even for a molecule as small as water.

Effect of pH and Temperature on Equilibrium Swelling. Figure 9(a) shows the equilibrium swelling fraction of SA-PAVA hydrogels in various pH meadia at 25 °C. Due to the effects of ionic strength, the equilibrium swelling fraction of the hydrogels in pH media were entirely smaller than those in DD water. It is well known that while NVC does not respond to changes in pH, AGA is a typical pH- sensitive polymeric chains that can deprotonate its carboxyl moieties in basic media and protonate them in acidic media. In addition, the extent of ionization of the carboxylic groups of SA, which produces greater number of carboxylate ions along the SA polymer chains, grows with the increasing pH value of the swelling medium from pH 1 to 5. These carboxylate ion centers repel each other and produce a rapid relaxation in the hydrogel network chains, thus resulting in a rise in the degree of fluid uptake. The slight increase in the swelling equilibrium in the range of pH values from 1 to 5 is maintained probably due to the action of buffer. At the maximum point (pH 7 to 9), all the -COOH groups of SA and AGA are converted to COO^-, resulting in high anion-anion repulsion and high swelling capacity. The decrease in the swelling in the medium of pH values above 7 may be explained in the light of the fact that at higher alkaline range the carboxylic groups of the SA molecules undergo dissociation resulting in the weakening of the physical forces between SA and AGA.

Effect of temperature on the swelling behavior of SA-PAVA hydrogels are shown in Figure 9(b). The swelling fraction of SA-PAVA hydrogels decrease with increasing temperature of the swelling media. In general swelling behavior of thermo responsive hydrogels are influenced by the temperature of swelling media. It is a quite known fact that PNVC containing hydrogels have LCST behavior. At temperatures below the LCST hydrogen bonds between water molecules and hydrophilic groups give the hydrogels good swellability. When the external temperature is increased to the LCST, the hydrogen bonds are overcome by the hydrophobic interactions among the hydrophobic groups, causing phase separation and shrinkage of the hydrogel nework.[34-37] The SA-PAVA semi-IPN hydrogels became swollen at temperatures below the LCST, but underwent a deswelling process when the external temperature was increased.

From Figure 9(b) it is observed that the swelling fraction of

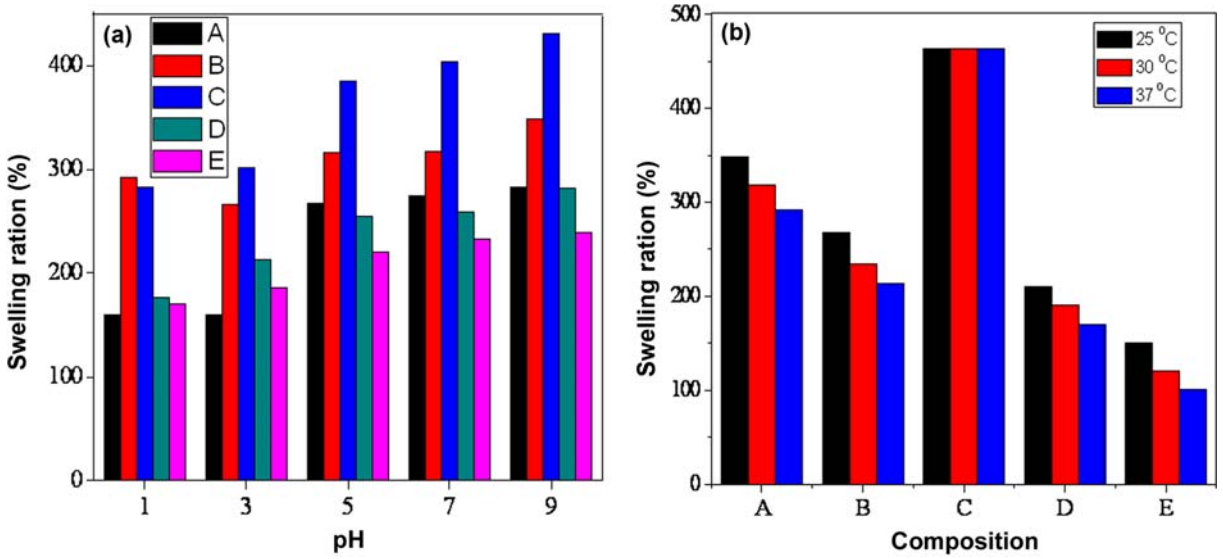

Figure 9. Effect of (a) pH and (b) temperature on equilibrium swelling ratio of different semi-IPN hydrogels; Formulations A, B, C, D, and E are listed in Table I.

A is smaller than B due to the shrinking effect of A having more crosslinking than B. The swelling fraction of B is smaller than C due to the presence of B containing a thermo sensitive monomer. But C has no thermo sensitive monomer and thus the swelling fraction of C is larger than A and B. Swelling fraction of D and E are also smaller than the composition A due to the smaller polymer concentration in hydrogel.

Drug Delivery. SA-PAVA hydrogel networks were used as a controlled release of 5-FU, anti cancer drug. 5-FU was encapsulated into the hydrogels by equilibrium swelling in 5-FU solution and followed by drying. In general, the dried hydrogels absorb water, likewise the 5-FU was transported with water due to the concentration gradient of 5-FU between the outside and inside regions of the hydrogel. The percentage of encapsulation efficiencies of 5-FU in SA-PAVA hydrogel are in the range 23.66% to 57.12%. Figure 10(a) shows the release profiles of SA-PAVA hydrogels cross-linked with different amounts of monomers containing 5-FU in pH 7.4 buffer medium. The % cumulative release 5-FU release of SA-PAVA hydrogels showed an initial burst at a range 0 to 5 h, followed by a sustained burst at range 5-12 h, and a plateau at a range 12-25h. In the case of crosslinker concentration (BAm, 9.7×10^{-4} mol%), % cumulative release for the hydrogel is lower, while for the other case (BAm 8.1×10^{-4} mol%) the intermediate values were observed. This is due to a decrease in matrix swelling as a result of increased BAm content of SA-PAVA hydrogels. However, drug release from SA-PAVA hydrogels is attributed to the following mechanisms: (i) drug release from the surface of matrix, (ii) drug diffusion through the swollen rubbery matrix and (iii) drug release due to matrix erosion in the external environment. At the initial stage higher release rates were observed due to the dissolution of the surface-adhered 5-FU. At longer durations, the drug release is controlled by diffusion rather than erosion of the matrix, thus it becomes much slower when compared to the initial release rates. Among all formulations, formulation A exhibited 100% release of 5-FU within 25 h.

In Figure 10(b) and (c), the SA-PAVA hydrogels showed a pH-sensitive and temperature responsive release of 5-FU from hydrogels. At pH 1.2 small amounts of 5-FU were released from the hydrogels while at pH 7.4 relatively large amounts of 5-FU were released from the hydrogels. The release of

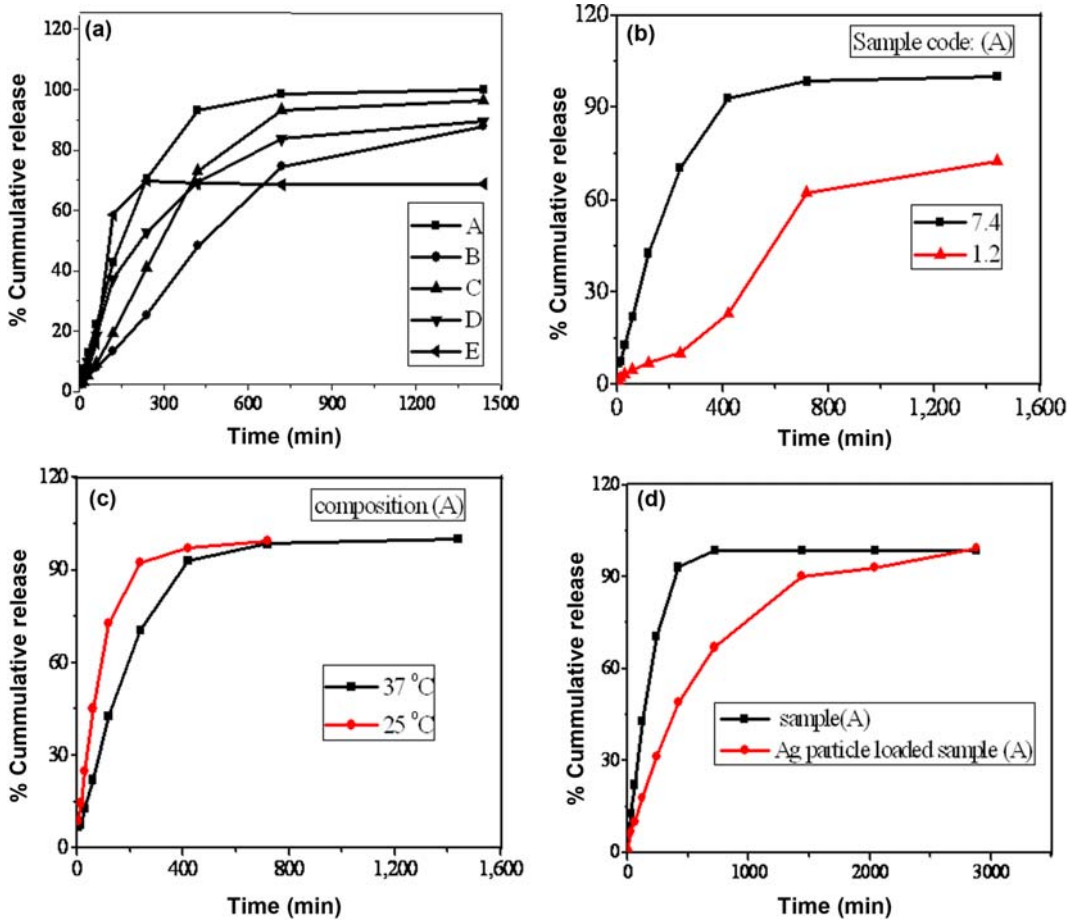

Figure 10. % Cumulative release of 5-FU through (a) different semi-IPN hydrogels at pH 7.4, (b) sample (A) semi-IPN hydrogel at pH 7.4 and 1.2, (c) sample (A) semi-IPN hydrogel at 37 and 25 °C, and (d) silver particle loaded sample (A) hydrogel at pH 7.4; Formulations A, B, C, D, and E are listed in Table I.

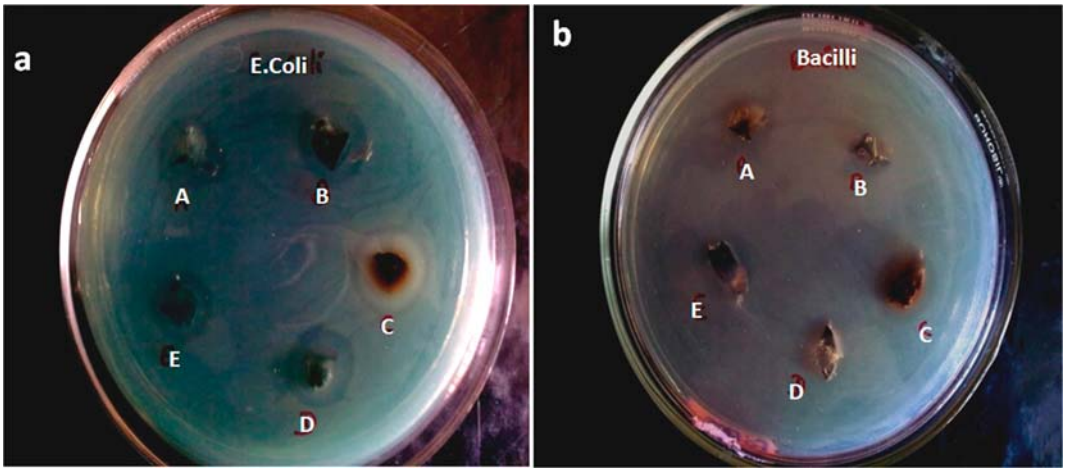

Figure 11. Representative photographs for the bactericidal activity of sodium alginate-based silver nanoparticles toward (a) *E. coli* and (b) *Bacilli*; Formulations A, B, C, D, and E are listed in Table I.

Table I. Feed Composition of Different Formulations[a]

Sample Code	SA (mL)	AGA×10^{-2} (mol)	NVC×10^{-2} (mol)	BAm×10^{-4} (mol)	% EE	*n*	r^2	*K*
A	2.5	1.5	1.8	8.1	50.941.1	0.649	0.939	1.72
B	2.5	0.0	1.8	8.1	48.520.8	0.551	0.939	0.97
C	2.5	1.5	0.0	8.1	57.121.3	0.740	0.946	0.55
D	2.5	1.5	1.8	9.7	53.690.5	0.765	0.991	0.83
E	0.0	1.5	1.8	8.1	23.661.6	0.868	0.926	0.59

[a]Am: 1 g, KPS 3.7×10^{-3} mol for all formulations; %EE= % encapusation efficiency.

5-FU is high at 25 ºC than 37 ºC. This is due to the temperature responsive behavior of poly(vinyl caprolactam). The release of 5-FU from the hydrogel matrix depends upon the swelling behavior of hydrogels. As explained clearly in the swelling experiments. Figure 10(d) gives the information of the effect of the silver nanoparticles on 5-FU release from the SA-PAVA-Ag nanocomposite of the sample A. The results indicated that the release of 5-FU is high when compared to the SA-PAVA hydrogel due to the formation of voids, during the formation of silver nanoparticles in the network.

Antimicrobial Study. The synthesized SA-PAVA-Ag nanocomposites were assayed for antibacterial activity against *Escherichia coli* and *Bacilli* by using a disc diffusion method. As shown in Figure 11(a), the silver nanoparticles showed zone of inhibition against all the studied bacteria. Maximum zone of inhibition was found in *Escherichia coli* and intermediate activity was revealed against *Bacilli* (Figure 11(b)). Metal nanoparticles are injurious to bacteria and fungi.[38] Silver nanoparticles possess well developed surface chemistry, chemical stability and appropriate smaller size, which make them easier to interact with the microorganisms.[19] The enhanced activity might be due to the nano size of silver nanoparticles, large surface area and high penetrating power. Hence, such nanoparticles could effectively bind to the substrates on the outer membrane and cell membrane of organisms.

Conclusions

In conclusion, 5-fluorouracil molecules can be encapsulated inside of SA-PAVA hydrogel network. In addition, well-dispersed and stable silver nanoparticles were fabricated inside SA-PAVA hydrogel networks. Thermal and UV-visible spectra analysis revealed the formation of silver nanoparticles in the hydrogel matrices. SEM and TEM images showed the narrow distribution and spherical shapes of silver nanoparticles in the hydrogel network. Furthermore, we proved that controlled release property of our SA-PAVA hydrogel network system could be easily controlled by pH, temperature and silver nanoparticles. Hence, we conclude that the hydrogels and hydrogel SNCs investigated in this study are potential candidates for drug delivery and antimicrobial applications, respectively.

Acknowledgments. Dr. K.S.V. Krishna Rao and Mr. P. Rama Subba Reddy thank to the Department of Science and technology (DST), New Delhi, India, (DST No.SR/FT/CS-047/2009) for a financial support. CSH thanks for the financial support to the National Research Foundation of Korea through the Ministry of Science, ICT & Future Planning, Korea (Korea-Russia (NRF-RFBR) Joint Research Program (No. 2013K2A1A7076267); Pioneer Research Center Program (No. 2010-0019308/2010-

0019482)) and Brain Korea 21 Plus program (21A2013800002)).

Supporting Information: Information is available regarding the TGA characterization of hydrogel and silver nanocomposite hydrogels for formulations B, C, D, and E. The materials are available *via* the Internet at http://www.springer.com/13233.

References

(1) D. S. W. Benoit, S. D. Collins, and K. S. Anseth, *Adv. Funct. Mater.,* **17**, 2085 (2007).
(2) A. Shikanov, R. M. Smith, M. Xu, T. K. Woodruff, and L. D. Shea, *Biomaterials*, **32**, 2524 (2011).
(3) G. Chen and A. S. Hoffman, *Nature*, **373**, 49 (1995).
(4) T. Gao, W. Wang, and A. Wang, *Macromol. Res.,* **19**, 739 (2011).
(5) J. T. Zhang, S. X. Cheng, S. W. Huang, and R. X. Zhuo, *Macromol. Rapid Commun.,* **24**, 447 (2003).
(6) D. P. Huynh, C. T. Huynh, and D. S. Lee, *Macromol. Res.,* **18**, 589 (2010).
(7) H. Savas and O. Guven, *Int. J. Pharm.,* **224**, 151(2001).
(8) K. Joseph and L. Robert, *Adv. Drug Deliv. Rev.,* **46**, 125 (2001).
(9) N. Orakdogen, *Macromol. Res.,* **22**, 32 (2014).
(10) X. Z. Zhang, D. Q. Wu, and C. C. Chu, *Biomaterials,* **25**, 3793 (2004).
(11) E. Jabbari and S. Nozari, *Eur. Polym. J.* **36**, 2685 (2000).
(12) I. Kaetsu, K. Uchida, H. Shindo, S. Gomi, K. Sutani, *Radiat. Phys. Chem*., **55**, 193 (1999).
(13) K. S. V. Krishna Rao, B. V. K. Naidu, M. C. S. Subha, and T. M. Aminabhavi, *Carbohydr. Polym.,* **66**, 333 (2006).
(14) X. Li, W. Wu, J. Wang, and Y. Duan, *Carbohydr. Polym.,* **66**, 473 (2006).
(15) B. L. Guo and Q. Y. Gao, *Carbohydr. Res.,* **342**, 2416 (2007).
(16) K. M. Reddy, V. R. Babu, K. S. V. K. Rao, M. C. S. Subha, K. C. Rao, M. S. Ram, and T. M. Aminabhavi, *J. Appl. Polym. Sci.,* **107**, 2820 (2008).
(17) A. L. Carmen, A. Concheiro, S. D. Alexander, N. V. Grinberg, T. V. Burova, and V. Y. Grinberg, *J. Control. Release*, **102**, 629 (2005).
(18) T. S. Cu, V. D. Cao, C. K. Nguyen, and N. Q. Tran, *Macromol. Res*., **22**, 418 (2014).
(19) K. S. V. K. Rao, P. R. Reddy, Y. I. Lee, and C. Kim, *Carbohydr. Polym*., **87**, 920 (2012).
(20) Y. Kim, V. R. Babu, D. T. Thangadurai, K. S. V. K. Rao, H. Cha, C. Kim, W. Joo, and Y. I. Lee, *Bull. Korean Chem. Soc.*, **32**, 553 (2011).
(21) W. R. Gombotz and S. F. Wee, *Adv. Drug Deliv. Rev.,* **31**, 267 (1998).
(22) A. Kikuchi, M. Kawabuchi, A. Watanabe, M. Sugihara, Y. Sakurai, and T. Okano, *J. Control. Release*, **58**, 21 (1999).
(23) I. Y. U. Galaev and B. Mattiasson, *Enzyme Microb. Technol.,* **15**, 354 (1993).
(24) Y. Liu, L. J. Duan, M. J. Kim, J. H. Kim, and D. J. Chung, *Macromol. Res.*, **22**, 240 (2014).
(25) K. S. V. K. Rao, A. B. V. K. Kumar, K. M. Rao, M. C. S. Subha, and Y. I. Lee, *Polym. Bull.,* **61**, 81 (2008).
(26) A. C. W. Lau and C. Wu, *Macromolecules*, **32**, 581 (1999).
(27) H. Vihola, A. Laukkanen, L. Valtola, H. Tenhu, and J. Hirvonen, *Biomaterials,* **26**, 3055 (2005).
(28) K. S. V. K. Rao and C. S. Ha, *Polym. Bull.,* **62**, 167 (2009).
(29) X. F. Li, X. Q. Feng, S. Yang, T. P. Wang, and Z. X. Su, *Iran. Polym. J.,* **17**, 843 (2008).
(30) S. Waxman and K. J. Scanlon, in *Clinical Interpretation and Practice of Cancer Chemotherapy*, E. M. Greenspan, Ed., Raven press, New York, 1982, p 38.
(31) J. P. Sommadossi, D. A. Gewirtz, R. B. Diasio, C. Aubert, J. P. Cano, and I. D. Goldman, *J. Biol. Chem.*, **257**, 8171 (1982).
(32) S. Einmahl, M. Zignani, E. Varesio, J. Heller, J. L. Veuthey, C. Tabatabay, and R. Gurny, *Int. J. Pharm.,* **185**, 189 (1999).
(33) N. Aggarwal, H. Hogen Esch, P. Guo, A. North, M. Suckow, and S. K. Mittal, *Can. J. Vet. Res.,* **63**, 148 (1999).
(34) O. Garcia, R. M. Trigo, M. D. Blanco, and J. M. Teijon, *Biomaterials*, **15**, 689 (1994).
(35) H. Inomato, S. Goto, and S. Saito, *Macromolecules*, **23**, 4887 (1990).
(36) T. Tokuhiro, T. Amiya, A. Mamada, and T. Tanaka, *Macromolecules*, **24**, 2936 (1991).
(37) R. Yoshida, Y. Okuyama, K. Sakai, T. Okano, and Y. Sakurai, *J. Membr. Sci.,* **89**, 267 (1994).
(38) H. E. Sherif, M. E. Masry, and A. Kansoh, *Macromol. Res.*, **19**, 1157 (2011).